HUMAN BIOLOGY
2024, VOL. 94, ISSUE 4
ORIGINAL ARTICLE

OPEN ACCESS

Whole-Volume Apparent Diffusion Coefficient Histogram Analysis for Prediction of Lymph Node Metastasis in Periampullary Carcinomas

Lei Bi [1,2], Wei Chen[3], Shijuan Zhou[2], Hongzhi Xu[4], Yushuai Lin[1], Juntao Zhang[5], Xiaodong Li [2], Ximing Wang[1*].*

ABSTRACT

Background: To evaluate whether whole-volume apparent diffusion coefficient (ADC) histogram parameters of the primary tumor were useful to predict regional lymph node metastasis (LNM) in periampullary carcinomas.

Methods: Thirty-eight patients with periampullary carcinoma who underwent pancreaticoduodenectomy between January 2016 to April 2019 were retrospectively enrolled. Whole-volume ADC histogram analysis of the primary tumor was performed by two radiologists independently. Clinical factors, pathological results and histogram parameters were recorded and evaluated. Intraclass correlation coefficient (ICC) was used to assess agreement between observers. Receiver operating characteristic (ROC) analysis was performed to evaluate the performance of parameters in differentiating LNM-positive group and LNM-negative group.

Results: Interobserver agreements were good to excellent for histogram analysis between two radiologists, with ICCs ranging from 0.766 to 0.967. Tumor size, MR-reported LN status and most ADC histogram parameters (including mean, minimum ADC value, 10th, 25th, 50th, 75th, and 90th percentile, and kurtosis) were significantly different between LNM-positive group and LNM-negative group ($p < 0.05$), and revealed significant correlations with LNM ($p < 0.05$). At ROC analysis, tumor size and minimum ADC value generated highest area under the curve (AUC) (AUC = 0.764, 95% confidence interval [CI]: 0.599, 0.886). When diagnostic predictive values were calculated with the combined model incorporating tumor size, MR-reported LN status and 75th percentile, the best diagnosis performance was obtained, with AUC of 0.879 (95% CI: 0.771, 0.986), sensitivity of 100.0%, and specificity of 75.0%.

Conclusion: Whole-volume ADC histogram parameters of the primary tumor held great potential in differentiating regional LNM in periampullary carcinomas.

INTRODUCTION

Periampullary carcinomas (PCs) constitute a rare heterogeneous group of malignant tumors originating from pancreas, distal common bile duct, duodenum, and ampulla of Vater. These tumors arise within 2 cm of the major duodenal papilla, and share a common embryologic origin from the foregut Bi et al. (2016). Although rare, accounting for roughly 0.2% of gastrointestinal tumors He et al. (2018), Yeo et al. (1998), Zakaria et al. (2020), PC is one of the top five leading causes of cancer-related death worldwide Malvezzi et al. (2016), with the detection rate increasing year by year Siegel et al. (2021). Pancreaticoduodenectomy remains the only potential curative option for resectable PCs, however, when first diagnosed, nearly 70%-80% of the patients have lost the opportunity for surgery because of lymph node metastasis (LNM), adherent tissues or vessels invasion, and distant metastasis Raj et al. (2013). Even the tumor was completely resected, the patients' prognosis is still poor due to the local recurrence and/or distant metastases after surgery Chen et al. (2013), Nakeeb et al. (2018).

Patients with PC were prone to be accompanied by LNM, which was reported to be one of the strongest risk factors for poor survival Chen et al. (2013), Nakeeb et al. (2018), Wennerblom et al. (2018). Previous study showed that the prognosis of patients with LNM was significantly worse than patients without LNM Nappo et al. (2015).

[1]Department of Radiology, Shandong Provincial Hospital Affiliated to Shandong First Medical University, Jinan, China
[2]Department of Radiology, Linyi People's Hospital, Linyi, China
[3]School of Radiology, Shandong First Medical University, Jinan, China
[4]Department of Ultrasonics, Linyi People's Hospital, Linyi, China
[5]Precision Health Institution, GE Healthcare, Shanghai, China

Correspondence to: Xiaodong Li, Department of Radiology, Linyi People's Hospital, No. 27, Jiefang Road, Lanshan District, Linyi, China, 276002. Telephone: +86 13605390909. Email: lxd8199819@126.com.

Ximing Wang, Department of Radiology, Shandong Provincial Hospital Affiliated to Shandong First Medical University, No. 324, Jingwu Road, Huaiyin District, Jinan, China, 250012. Telephone: +86 15168886672. Email: wxming369@163.com.

Keywords: periampullary carcinoma, ADC, histogram, lymph node metastasis

What's more, Kim et al found that if patients with LNM received neoadjuvant chemotherapy before surgery, through the fiborsis of metastastic LNs, patient's prognosis could be improved Kim et al. (2016). Therefore, accurate preoperative evaluation of LN status is crucial for selecting optimal individualized treatment strategy, and could assist to predict patients' prognosis.

Diffusion-weighted imaging (DWI) is a non-invasive MRI technique to measure molecular Brownian movement inside tissues, and is quantified by the apparent diffusion coefficient (ADC) Meyer et al. (2021). ADC values were proved to be associated with tumor cellularity, proliferation potential, neoangiogenesis, lymphocytes and extracellular matrix invasion Meyer et al. (2021), which can be used to distinguish benign and malignant neoplasmas, predict patient prognosis, and assess tumor response to treatment Bi et al. (2016). Recently, ADC histogram analysis has received extensive recognition as a reproducible approach which can reflect the heterogeneity of molecular diffusion within a tumor region based on pixel distribution Nakajo et al. (2018). ADC histogram analyses have yielded great potential for predicting LNM in various malignant tumors, such as gastric cancer Liu et al. (2017), colorectal cancer Zhou et al. (2021), Li et al. (2021), Nerad et al. (2019), uterine cervical cancer Lee et al. (2020), and epithelial ovarian cancer Wang et al. (2019). Till now, there has been no published research that has evaluated whether whole-volume ADC histogram analysis would facilitate LNM prediction in PCs.

Therefore, the purpose of our study was to assess the diagnostic potential of ADC histogram analysis for predicting LNM of PCs.

MATERIALS AND METHODS

Study population

This retrospective study of anonymous data was approved by the Ethics Committee of our institution, and requirement for informed consent was waived. Preoperative MR images of patients with PC were searched from our database. The inclusion criteria included: 1) patients were treated with curative whole-tumor resection and lymphadenectomy; 2) comprehensive clinical and pathological results were available; 3) time interval between preoperative MR examination and surgery was less than two weeks; and 4) ADC maps had high quality (without artifacts) for segmentation. The exclusion criteria included: 1) patients received radiotherapy or chemotherapy before surgery; and 2) patients suffered from other malignancies simultaneously. From January 2016 to April 2019, a total of 38 patients (mean age, 54.6 years; range, 38-72 years), including 21 men (mean age, 57.2 years; range, 41-72 years) and 17 women (mean age, 52.0 years; range, 38-70 years) were included in our study (Figure 1).

Figure 1: Flow diagram of patient selection procedure. ADC = apparent diffusion coefficient.

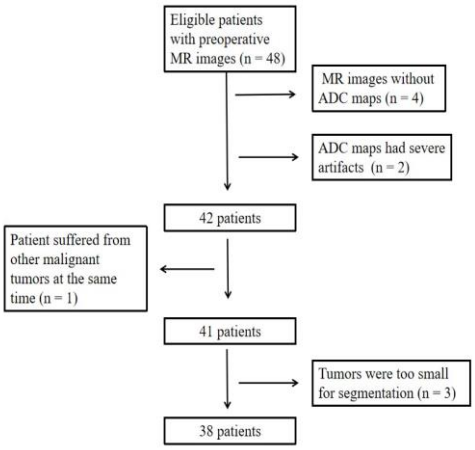

MRI examinations

MRI examinations were performed on a 3.0-T MRI system (Magnetom Verio, Siemens) using an eight-channel phased-array surface coil. Parallel acquisition technique and retrospective image intensity correction (B1 filter) were used to reduce standing wave or dielectric effects. A respiratory-triggered, fat-suppressed, single-shot echo-planar imaging in the transverse position was performed for DWI sequence. Each acquisition was obtained using b values of 0 and 800 s/mm2. The overall acquisition time ranged from 3 to 6 minutes depending on patient's respiratory efficiency. ADC map was generated automatically with a commercially available software workstation system (Syngo Multimodality workplace, Siemens). The acquisition parameters of DWI sequence were as follows: TR/TE = 4000/73 ms; field of view = 380 mm × 285 mm; flip angle = 90^0; matrix = 128 × 78; slice thickness = 5 mm; band width = 2442 Hz/pixel; ETL = 78; echo space = 0.51 ms.

In addition to DWI, routine MRI including a T1-weighted dual-echo in- and out-phase sequence, a T1-weighted volume interpolated body examination (VIBE) sequence, and a breath-hold turbo spin-echo T2-weighted sequence were performed before administration of contrast agent. For enhanced imaging, arterial phase (20-25 sec), portal venous phase (60-70 sec), equilibrium phase (3 min), delayed phase (10 min) and hepatobiliary phase (90 min) were obtained using VIBE sequence after injection of gadobenate dimeglumine. With a power injector, the contrast agent was administered intravenously at a rate of 2.5 mL/s for a total dose of 0.1 mmol/kg of body weight, followed by a 20-mL saline flush.

MR feature evaluation

Two radiologists (observer 1 and observer 2, with 8 and 15 years of experience in abdominal MR interpretation, respectively) reviewed all images in consensus.

The following image features were evaluated: 1) tumor size, defined as the lesion's maximum diameter on axial images; 2) vascular involvement, defined as vessel occlusion, stenosis, or contour deformity due to tumor invasion; and 3) LNM, defined as LN's short-axis diameter larger than 10 mm, or LNs with central necrosis, or LNs were hyperenhanced than liver parenchyma in portal venous phase Ji et al. (2019), Bi et al. (2021).

The observers knew that all patients were diagnoses of PC but were blind for the clinical and pathological details.

Tumor segmentation and histogram analysis

Three-dimensional segmentation was performed using ITK-SNAP (v. 3.8.0). Two radiologists performed the tumor segmentation independently. On ADC map, the region of interest (ROI) was manually drawn freehand on each transverse section strictly within the border of the lesion layer by layer, which should include cyst, hematoma, or necrosis within the lesion, but avoid common bile duct, main pancreatic duct and other normal anatomical structures. The ROIs were first localized on DWI with reference to T1-weighted, T2-weighted, and gadolinium-enhanced VIBE images, and mirrored to the ADC maps subsequently.

The volume of interest (VOI) of each lesion was then automatically generated for histogram analysis (Figure 2).

Figure 2: Histogram analyses on apparent diffusion coefficient (ADC) maps of periampullary carcinomas in a 48-year-old woman with lymph node metastasis

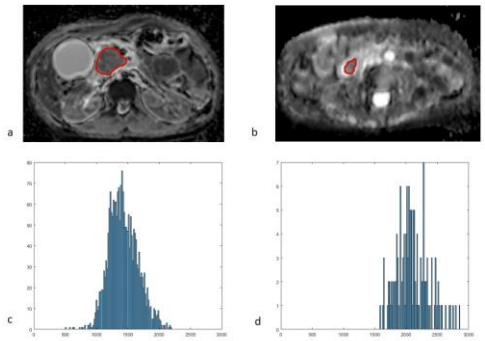

(a) and a 65-year-old woman without lymph node metastasis (b). On ADC map, the region of interest was manually drawn freehand on each transverse section strictly within the border of the lesion. After whole-volume segmentation, the histogram of gray-level distribution was generated (c, d).

PyRadiomics (v. 3.1.0) was used for feature extraction. Various first-order parameters including quartiles (25th, 50th, 75th), 10th and 90th percentiles, maximum, minimum and mean ADC values, energy, kurtosis, variance, and skewness were obtained.

Pathological diagnosis of LNM

All the patients underwent lymphadenectomy. The resected LN areas included peripancreatic, retropancreatic, hepatoduodenal, celiac, superior mesenteric, portocaval, and aortocaval. Resected LNs of each area were grouped and sent for histopathological examination. LNM means that at least one of the LNs was positive.

Statistical analysis

Univariate analysis was applied to compare the differences in the clinical factors and ADC histogram parameters between LNM-positive group and LNM-negative group. Categorical variables were compared by using Chi-square test or Fisher exact test, and continuous variables were compared by using Student's t test or Mann-Whitney U test, as appropriate. Interobserver agreement was assessed by using interclass correlation coefficient (ICC). An ICC value of 1.0 was deemed to indicate perfect agreement; 0.81-0.99, excellent correlation; 0.61-0.80, good correlation; 0.41-0.60, moderate agreement; 0.21-0.40, fair correlation; and 0.20 or less, poor correlation Landis et al. (1977). Spearman correlation analysis was done to assess the correlation between variables and LN metastasis. Diagnostic performance of variables for differentiating two groups was calculated by using receiver operating characteristic (ROC) curve analysis, and the evaluation indicators included area under the curve (AUC), sensitivity, and specificity. The optimal cutoff value was defined according to Youden index (the value at which the sum of the sensitivity and specificity was maximized). Multivariate model calibration was assessed with the goodness-of-fit Hosmer-Lemeshow test through a calibration plot. All statistical analyses were performed using SPSS software (SPSS for Windows, v. 17.0; Chicago, IL) and MedCalc software (MedCalc for Windows, v. 12.7.0; Mariakerke, Belgium). A p-value < 0.05 was considered statistically significant.

RESULTS

Patient demographics

Among the 38 patients in our study, 10 patients (5 men, 5 women; mean age, 48.0 years; range, 47-69 years) were diagnosed with LNM, and 28 patients (16 men, 12 women; mean age, 55.6 years; range, 38-72 years) without LNM. In total, 5 patients (50.0%; 5 of 10) with LNM were understaged, and 3 patients (10.7%; 3 of 28) without LNM were overstaged based on MR-reported LN status. Nine tumors (23.7%) were located at duodenum, 6 (15.8%) at ampulla of Vater, 5 (13.1%) at common bile duct, and 18 (47.4%) at pancreas. Pathological reports showed that 3 tumors (7.9%) were well differentiated, 23 (60.5%) were moderately differentiated, and 12 (31.6%) were poorly differentiated (Table 1).

Table 1: Patient and tumor characteristics

Characteristic	LNM-positive group (n = 10)	LNM-negative group (n = 28)	p value
Age (mean ± SD)	56.00 ± 7.23	55.86 ± 10.28	0.968
Gender			0.697
Male	5 (50.0)	16 (57.1)	
Female	5 (50.0)	12 (42.9)	
Tumor size (mean ± SD)	3.68 ± 1.09	2.63 ± 1.21	0.02
MR-reported LN status			0.009
LNM-positive	5 (50.0)	3 (10.7)	
LNM-negative	5 (50.0)	25 (89.3)	
Vascular involvement	3 (30.0)	2 (7.1)	0.066
Tumor origin			0.306
Duodenum	2 (20.0)	7 (25.0)	
Ampulla of Vater	3 (30.0)	3 (10.7)	
Common bile duct	0 (0.0)	5 (17.9)	
Pancreas	5 (50.0)	13 (46.4)	
Degree of differentiation			0.502
High	0 (0.0)	3 (10.7)	
Moderate	6 (60.0)	17 (60.7)	
Low	4 (40.0)	8 (28.6)	

Note: Data are number of patients; data in parentheses are percentage unless otherwise indicated. LN, lymph node; LNM, lymph node metastasis; MR, magnetic resonance; SD, standard deviation.

Univariate analysis

1. Comparison of clinical and pathological characteristics

The tumor size and MR-reported LN status were significantly different between LNM-positive group and LNM-negative group ($p = 0.020$ and 0.019, respectively), and revealed significantly positive correlations with LN metastasis ($rs = 0.406$, $p = 0.011$, and $rs = 0.424$, $p = 0.008$, respectively). The other parameters did not differ significantly between two groups ($p > 0.05$) (Table 1).

2. Comparison of ADC histogram parameters

Interobserver agreements of histogram parameters were good to excellent, with ICCs ranging from 0.766 to 0.967 (Table 2).

The mean, minimum ADC values and 10th, 25th, 50th, 75th, and 90th percentile values were significantly lower in LNM-positive group than in LNM-negative group ($p = 0.014$-0.047), and revealed significantly negative correlations with LN metastasis ($rs = -0.403$-$[-0.327]$, all $p < 0.05$). The kurtosis was significantly higher in LNM-positive group than in LNM-negative group ($p = 0.028$), and had a positive correlation ($rs = 0.360$, $p = 0.027$) with LN metastasis. The other parameters did not differ significantly between two groups ($p > 0.05$) (Table 3).

ROC analysis

1. Diagnostic performances of clinical and pathological characteristics. The tumor size generated highest AUC in all clinical and pathological parameters for

Table 2: Interobserver Agreement for the Measurement of ADC Histogram Parameters

Histogram parameters	ICC (95% CI)
10th percentile ADC	0.938 (0.915, 0.961)
25th percentile ADC	0.933 (0.912, 0.953)
Median ADC	0.923 (0.901, 0.945)
75th percentile ADC	0.917 (0.890, 0.944)
90th percentile ADC	0.917 (0.892, 0.942)
Minimum ADC	0.967 (0.927, 1.000)
Mean ADC	0.936 (0.918, 0.953)
Maximum ADC	0.935 (0.874, 0.995)
Energy	0.911 (0.886, 0.936)
Kurtosis	0.766 (0.663, 0.868)
Variance	0.871 (0.819, 0.924)
Skewness	0.793 (0.722, 0.864)

Note: ADC, apparent diffusion coefficient; CI, confidence interval; ICC, interclass correlation coefficient.

Table 3: Histogram parameters between the LNM-positive and LNM-negative groups and ROC curve results

Histogram parameters	LNM-positive group	LNM-negative group	p value	AUC (95% CI)	Sensitivity (%)	Specificity (%)	Correlation with LN status (rs)	p value of correlation test
10th percentile ADC (× 10-6 mm2/sec)	999 ± 258	1210 ± 339	0.044	0.718 (0.549, 0.851)	80	60.7	-0.332	0.041
25th percentile ADC (× 10-6 mm2/sec)	1111 ± 268	1327 ± 330	0.047	0.714 (0.545, 0.849)	40	100	-0.327	0.045
Median ADC (× 10-6 mm2/sec)	1243 ± 288	1482 ± 327	0.034	0.729 (0.560, 0.860)	80	64.3	-0.349	0.032
75th percentile ADC (× 10-6 mm2/sec)	1379 ± 258	1646 ± 333	0.014	0.761 (0.595, 0.884)	80	75	-0.398	0.013
90th percentile ADC (× 10-6 mm2/sec)	1531 ± 301	1803 ± 357	0.019	0.750 (0.583, 0.876)	80	67.9	-0.381	0.018
Minimum ADC (× 10-6 mm2/sec)	699 ± 292	1002 ± 443	0.013	0.764 (0.599, 0.886)	90	64.3	-0.403	0.012
Mean ADC (× 10-6 mm2/sec)	1259 ± 280	1497 ± 324	0.026	0.739 (0.572, 0.868)	80	64.3	-0.365	0.024
Maximum ADC (× 10-6 mm2/sec)	2166 ± 452	2200 ± 484	0.961	0.507 (0.340, 0.673)	20	53.6	-0.011	0.948
Energy (× 10-6)	981 ± 129	558 ± 810	0.172	0.650 (0.478, 0.797)	70	64.3	0.229	0.167
Kurtosis	4.66 ± 2.27	3.18 ± 1.09	0.028	0.736 (0.568, 0.865)	80	64.3	0.36	0.027
Variance (× 10-6)	0.052 ±0.019	659 ± 498	0.66	0.550 (0.380, 0.711)	100	32.1	-0.076	0.649
Skewness	0.69 ± 0.59	0.35 ± 0.57	0.116	0.671 (0.500, 0.815)	100	35.7	0.262	0.113

Note: ADC, apparent diffusion coefficient; AUC, area under the curve; CI, confidence interval; LNM, lymph node metastasis; ROC, receiver operating characteristic.

differentiating LNM-positive group and LNM-negative group (AUC = 0.764, 95% confidence interval [CI]: 0.599, 0.886), with sensitivity of 70.0%, and specificity of 82.1%. MR-reported LN status also showed good discrimination capability, with AUC of 0.713, while the tumor location generated lowest AUC of 0.500. Discrimination capabilities of vascular involvement and degree of differentiation were unsatisfactory, with AUC of 0.614 and 0.589, respectively.

2. Diagnostic performances of ADC histogram parameters

The minimum ADC value generated highest AUC in all histogram parameters for differentiating LNM-positive group and LNM-negative group (AUC = 0.764, 95% confidence interval [CI]: 0.599, 0.886), with sensitivity of 90.0%, and specificity of 64.3%. The 75th, 90th percentiles, mean ADC value and kurtosis also showed good discrimination capability, with AUC of 0.761, 0.750, 0.739 and 0.736, respectively, while the maximum ADC value generated lowest AUC of 0.507.

3. Diagnostic performances of combined models

When diagnostic predictive values were calculated with the combined model incorporating MR-reported LN status and 75th percentile, the AUC increased to 0.843 (95% CI: 0.718, 0.968), with sensitivity of 90.0% and specificity of 71.4%. When incorporating tumor size, MR-reported LN status and 75th percentile, the best diagnosis performance was obtained (AUC = 0.879, 95% CI: 0.771, 0.986), with sensitivity of 100.0% and specificity of 75.0%. A non-significant statistic (p = 0.490) of the Hosmer-Lemeshow test suggested no significant deviation from an ideal fitting. The ROC curve analyses were showed in Figure 3, and the diagnostic performance of parameters were presented in Table 3.

Figure 3: Receiver operating characteristic curves for diagnostic performance in differentiating lymph node metastasis (LNM)-positive group from LNM-negative group periampullary carcinomas. ADC = apparent diffusion coefficient, AUC = area under the receiver operating characteristic curve.

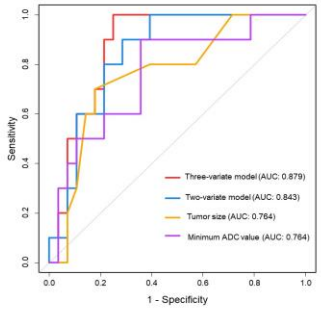

DISCUSSION

In this study, we investigated the diagnostic value of whole-volume ADC histogram analysis in predicting regional lymph node metastasis of periampullary carcinomas. Our results showed that most ADC histogram parameters were significantly different between LNM-positive group and LNM-negative group. At ROC analysis, the tumor size and minimum ADC value generated highest AUC of 0.764. When diagnostic predictive values were calculated with the combined model incorporating tumor size, MR-reported LN status and 75th percentile, the best diagnosis performance was obtained, with AUC of 0.879, sensitivity of 100%, and specificity of 75%.

Due to the region's anatomical complexity, PCs remain a diagnostic and therapeutic challenge. Preoperative prediction of LNM has received extensive attention due to its prognostic significance and the essential role in patient management.

In daily clinical practice, image-based differentiation of metastatic LNs from nonmetastatic LNs mainly depends on morphological features and LN's sizes, which is inevitably subjective. Moreover, benign LNs with nonspecific inflammatory hyperplasia and metastatic LNs with small sizes also exist. Tseng et al revealed that diagnostic accuracy of conventional CT imaging in assessing PCs' LNM was less than 81% Tseng et al. (2014). In our present study, half of the patients (5 in 10 patients) with LNM were underestimated based on the conventional MR images. Therefore, conventional imaging modalities' performance in assessment of LN status is inadequate. It is necessary to explore some new method to reveal the histopathological characteristics of metastatic LNs.

Prithivi Raj et al found that PET-CT has a potential ability for detecting PC' s LNM. In their study, FDG-PET/CT showed a sensitivity of 71.4 % and specificity of 77.8 % for assessment of LNM with cutoff value SUV max ≥ 2.0. However, small lesions that are less than twice the imaging resolution would yield false negative results because of partial volume effect, and high cost of PET scans may limit its utility in clinical practice Ji et al. (2019). In one of our previous studies, we established and validated a radiomics nomogram for preoperatively predicting LNM in PCs. The results showed that the radiomics nomogram incorporating radiomics signature and CT-reported LN status obtained favorable discrimination and calibration ability in both training and validation set, with AUC of 0.853 for each set Bi et al. (2021). However, although the radiomics nomogram performed well, it was complicated and time-consuming, to some extent.

Histogram analysis is a rapidly-emerging noninvasive

method in the field of medical imaging, which is capable of quantitatively and objectively assessing tumor heterogeneity, regularity, and image roughness by evaluating the distribution of voxel gray levels without requiring additional invasive procedures Zhao et al. (2021). ADC histogram can reflect tissue components with different diffusion features inside the tumor, which was proved to have favorable repeatability and comprehensiveness Wang et al. (2019). LNM has been reported to be associated with ADC histogram parameters of the primary tumor Liu et al. (2017), Zhou et al. (2021), Li et al. (2021), Nerad et al. (2019), Lee et al. (2020), Wang et al. (2019), which is consistent with our results. ADC values based on water molecular diffusion can reflect the microenvironment of tissues. In general terms, acellular regions (such as cystic and necrotic components) that allow free water diffusion would yield higher ADC values, and highly cellular areas in which water diffusion is restricted by the intensive cell membranes always yield lower ADC values Nakajo et al. (2018), Subhawong et al. (2014), Shindo et al. (2016).

When the primary tumor progresses, the proliferative ability of the tumor cells and their metastatic capacity were enhanced by the changes of tumor microenvironment Wang et al. (2019), Woo et al. (2014). Therefore, patients with LNM showed lower ADC values than that without LNM.

In present study, we not only evaluated various ADC values, but also ADC histogram kurtosis, energy, variance and skewness, which is a more reproducible approach and reflected the distribution of ADC values Umanodan et al. (2017). In our study, tumors with LNM showed higher kurtosis than tumors without LNM. Kurtosis reflects the peakedness of the histogram distribution and measures the shape of the probability distribution Just et al. (2014). Higher kurtosis indicates that the distribution tended to have heavier tails or outliers, and the mass of the distribution was more concentrated in tumors with LNM. Previous research has showed that kurtosis of ADC histogram could predict LN status in thyroid cancer Schob et al. (2017). In addition, energy, variance and skewness have also been reported to be correlated with pathological characteristics. Higher energy reflects narrower distribution of intensity levels, higher variance reflects more heterogeneous distribution of ADC values, and higher skewness reflects more asymmetric distribution of ADC values Umanodan et al. (2017), Yang et al. (2019). However, in our study, energy, variance and skewness were not significantly different between LNM-positive and LNM-negative group. Further studies focusing on this topic should be proposed.

For manual tumor segmentation, how to ensure the reproducibility of histogram analysis is the most important issue. Reports suggested that compared with a representative single cross-sectional lesion segmentation, whole-tumor analysis was more reproducible because ADC values were depended on the selected regions of interest, subjective selection of single section would reduce inter- and intraobserver agreements Nakajo et al. (2018). What's more, since PCs are often heterogeneous, a single region of interest could not comprehensively reflect different pathological characteristics within the entire tumor.

Therefore, in our study, we explored whole-volume ADC histogram analysis, and an overall good interobserver agreement was obtained, with ICCs ranging from 0.766 to 0.967. This was in accordance with previous studies which revealed that whole-volume histogram analyses exhibited favorable repeatability in clinical practice Nakajo et al. (2018), Gourtsoyianni et al. (2017), Gerlinger et al. (2012).

There were several limitations to our study. First, even with strict inclusion criteria, selection bias inevitably existed because of the retrospective design of our study. Patients with an advanced stage who could not undergo surgery were excluded. Second, this was a single-center study and the sample size was relatively small, so the diagnostic criteria proposed in our study should be validated in another cohort. Finally, the tumor segmentation was manually done by the radiologists, and further computer algorithm-assistant automatic segmentation should be used.

In conclusion, whole-volume ADC histogram analysis of the primary tumor could be a promising and noninvasive method for predicting regional lymph node metastasis of periampullary carcinomas.

KEY POINTS

1. ADC histogram parameters of the primary tumor may help to assess LN status in periampullary carcinoma.

2. ADC histogram parameters of the primary tumor were significantly different between LNM-positive group and LNM-negative group in periampullary carcinoma.

3. When diagnostic predictive values were calculated with the combined model incorporating tumor size, MR-reported LN status and 75th percentile, the best diagnosis performance was obtained, with AUC of 0.879.

ABBREVIATIONS

ADC, apparent diffusion coefficient

AUC, area under the curve

CI, confidence interval

DWI, diffusion-weighted imaging

ICC, interclass correlation coefficient

LNM, lymph node metastasis

PC, periampullary carcinomas

ROC, receiver operating characteristic

ROI, region of interest

VIBE, volume interpolated body examination

VOI, volume of interest

REFERENCES

1.Bi L, Dong Y, Jing C, et al. 2016 Apr Differentiation of pancreatobiliary-type from intestinal-type periampullary carcinomas using 3.0T MRI. J Magn Reson Imaging. 43(4):877-86.

2.He C, Mao Y, Wang J, et al. 2018 Apr 18. Surgical management of periampullary adenocarcinoma: defining an optimal prognostic lymph node stratification schema. J Cancer. 9(9):1667-1679.

3.Yeo CJ, Sohn TA, Cameron JL, et al. 1998 Jun. Periampullary adenocarcinoma: analysis of 5-year survivors. Ann Surg. 227(6):821-31.

4.Zakaria H, Sallam AN, Ayoub II, et al. 2020 Aug 11. Prognostic factors for long-term survival after pancreaticoduodenectomy for periampullary adenocarcinoma. A retrospective cohort study. Ann Med Surg (Lond). 57:321-327.

5.Malvezzi M, Carioli G, Bertuccio P, et al. 2016 Apr. European cancer mortality predictions for the year 2016 with focus on leukaemias. Ann Oncol. 27(4):725-31.

6.Siegel RL, Miller KD, Fuchs HE, et al. 2021 Jan. Cancer Statistics, 2021 CA Cancer J Clin. 71(1):7-33.

7.Raj P, Kaman L, Singh R, et al. 2013 Jun. Sensitivity and specificity of FDG PET-CT scan in detecting lymph node metastasis in operable periampullary tumours in correlation with the final histopathology after curative surgery. Updates Surg. 65(2):103-7

8.Chen SC, Shyr YM, Wang SE. 2013 Dec. Longterm survival after pancreaticoduodenectomy for periampullary adenocarcinomas. HPB (Oxford). 15(12):951-7.

9.Nakeeb AE, Sorogy ME, Ezzat H, et al. 2018 Oct. Predictors of long-term survival after pancreaticoduodenectomy for peri-ampullary adenocarcinoma: A retrospective study of 5-year survivors. Hepatobiliary Pancreat Dis Int. 17(5):443-449.

10.Wennerblom J, Saksena P, Jönsson C, et al. 2018 Feb. Lymph node 8a as a prognostic marker for poorer prognosis in pancreatic and periampullary carcinoma. Scand J Gastroenterol. 53(2):225-230.

11.Nappo G, Borzomati D, Perrone G, et al. 2015 Nov. Incidence and prognostic impact of para-aortic lymph nodes metastases during pancreaticoduodenectomy for peri-ampullary cancer. HPB (Oxford). 17(11):1001-8.

12. Kim SM, Eads JR. 2016 Dec. Adjuvant and Neoadjuvant Therapy for Resectable Pancreatic and Periampullary Cancer. Surg Clin North Am. 96(6):1287-1300.

13.Meyer HJ, Höhn AK, Surov A. 2021 Jan 20. Relationships between apparent diffusion coefficient (ADC) histogram analysis parameters and PD-L 1-expression in head and neck squamous cell carcinomas: a preliminary study Radiol Oncol. 55(2):150-157.

14.Nakajo M, Fukukura Y, Hakamada H, et al. 2018 Feb 22. Whole-tumor apparent diffusion coefficient (ADC) histogram analysis to differentiate benign peripheral neurogenic tumors from soft tissue sarcomas. J Magn Reson Imaging.

15.Liu S, Zhang Y, Chen L, et al. 2017 Oct 2. Whole-lesion apparent diffusion coefficient histogram analysis: significance in T and N staging of gastric cancers. BMC cancer. 17(1):665.

16.Zhou Y, Yang R, Wang Y, et al. 2021 Nov 22. Histogram analysis of diffusion-weighted magnetic resonance imaging as a biomarker to predict LNM in T3 stage rectal carcinoma. BMC Med Imaging. 21(1):176.

17.Li J, Zhou Y, Wang X, et al. 2021 Apr 1. Histogram Analysis of Diffusion-Weighted Magnetic Resonance Imaging as a Biomarker to Predict Lymph Node Metastasis in T3 Stage Rectal Carcinoma. Cancer Manag Res. 13:2983-2993.

18.Nerad E, Pizzi AD, Lambregts DMJ, et al. 2019 Feb 5. The Apparent Diffusion Coefficient (ADC) is a useful biomarker in predicting metastatic colon cancer using the ADC-value of the primary tumor PloS One. 14(2):e0211830.

19.Lee J, Kim CK, Park SY. 2020 Apr. Histogram analysis of apparent diffusion coefficients for predicting pelvic lymph node metastasis in patients with uterine cervical cancer. MAGMA. 33(2):283-292.

20.Wang F, Wang Y, Zhou Y, et al. 2019 Aug. Apparent Diffusion Coefficient Histogram Analysis for Assessing Tumor Staging and Detection of Lymph Node Metastasis in Epithelial Ovarian Cancer: Correlation with p53 and Ki-67 Expression. Mol Imaging Biol. 21(4):731-739.

21.Ji GW, Zhang YD, Zhang H, et al. 2019 Jan. Biliary Tract Cancer at CT: A Radiomics-based Model to Predict Lymph Node Metastasis and Survival Outcomes. Radiology. 290(1):90-98.

22.Bi L, Liu Y, Xu J, et al. 2021 Jul 29. A CT-Based Radiomics Nomogram for Preoperative Prediction of Lymph Node Metastasis in Periampullary Carcinomas. Front Oncol. 11:632176.

23.Landis JR, Koch GG. 1977 Mar. The measurement of observer agreement for categorical data. Biometrics. 33(1):159-74.

24.Tseng DSJ, van Santvoort HC, Fegrachi S, et al. 2014 Dec. Diagnostic accuracy of CT in assessing extra-regional lymphadenopathy in pancreatic and peri-ampullary cancer: a systematic review and meta-analysis. Surg Oncol. 23(4):229-35.

25.Bi L, Liu Y, Xu J, et al. 2021 Jul 29. A CT-Based Radiomics Nomogram for Preoperative Prediction of Lymph Node Metastasis in Periampullary Carcinomas Front Oncol. 11:632176.

26.Zhao L, Liang M, Shi Z, et al. 2021 May. Preoperative volumetric synthetic magnetic resonance imaging of the primary tumor for a more accurate prediction of lymph node metastasis in rectal cancer. Quant Imaging Med Surg. 11(5):1805-1816.

27.Subhawong TK, Jacobs MA, Fayad LM. 2014 Sep-Oct. Diffusion-weighted MR imaging for characterizing musculoskeletal lesions. Radiographics. 34(5):1163-77.

28.Shindo T, Fukukura Y, Umanodan T, et al. 2016 Jan. Histogram Analysis of Apparent Diffusion Coefficient in Differentiating Pancreatic Adenocarcinoma and Neuroendocrine Tumor. Medicine (Baltimore). 95(4):e2574.

29.Woo S, Lee JM, Yoon JH, et al. 2014 Mar. Intravoxel incoherent motion diffusion-weighted MR imaging of hepatocellular carcinoma: correlation with enhancement degree and histologic grade. Radiology. 270(3):758-67.

30.Umanodan T, Fukukura Y, Kumagae Y, et al. 2017 Apr. ADC histogram analysis for adrenal tumor histogram analysis of apparent diffusion coefficient in differentiating adrenal adenoma from pheochromocytoma. J Magn Reson Imaging. 45(4):1195-1203.

31.Just N. 2014 Dec 9 Improving tumour heterogeneity MRI assessment with histograms. Br J Cancer. 111(12):2205-13.

32.Schob S, Meyer HJ, Dieckow J, et al. 2017 Apr 12. Histogram Analysis of Diffusion Weighted Imaging at 3T is Useful for Prediction of Lymphatic Metastatic Spread, Proliferative Activity, and Cellularity in Thyroid Cancer. Int J Mol Sci. 18(4):821.

33.Yang L, Liu D, Fang X, et al. 2019 Dec. Rectal cancer: can T2WI histogram of the primary tumor help predict the existence of lymph node metastasis? Eur Radiol. 29(12):6469-6476.

34.Gourtsoyianni S, Doumou G, Prezzi D, et al. 2017 Aug. Primary Rectal Cancer: Repeatability of Global and Local-Regional MR Imaging Texture Features. Radiology. 284(2):552-561.

35.Gerlinger M, Rowan AJ, Horswell S, et al. 2012 Mar 8. Intratumor heterogeneity and branched evolution revealed by multiregion sequencing. N Engl J Med. 366(10):883-892.

